Physiol Genomics 32: 142–153, 2007.
First published October 16, 2007; doi:10.1152/physiolgenomics.00258.2006.

Characterization and functional divergence of the α_1-adrenoceptor gene family: insights from rainbow trout (*Oncorhynchus mykiss*)

Xi Chen,[1] Steve F. Perry,[1] Stéphane Aris-Brosou,[1,2] Corrado Selva,[1] and Thomas W. Moon[1]

[1]*Department of Biology and Centre for Advanced Research in Environmental Genomics,* [2]*Department of Mathematics and Statistics, University of Ottawa, Ottawa, Ontario, Canada*

Submitted 22 November 2006; accepted in final form 10 October 2007

Chen X, Perry SF, Aris-Brosou S, Selva C, Moon TW. Characterization and functional divergence of the α_1-adrenoceptor gene family: insights from rainbow trout (*Oncorhynchus mykiss*). *Physiol Genomics* 32: 142–153, 2007. First published October 16, 2007; doi:10.1152/physiolgenomics.00258.2006.—Presently, three α_1-adrenoceptor (AR) types are recognized in vertebrates: α_{1A}-, α_{1B}-, and α_{1D}-ARs. These α_1-subtypes have distinct pharmacology and molecular profiles, play crucial roles in metabolic and vascular control, and are the targets for numerous pharmaceuticals, especially those affecting blood pressure and vascular resistance. To better understand the functional divergence within the α_1-AR gene family, we sequenced these α_1-AR paralogs in the rainbow trout and performed an extensive phylogenetic analysis. We show that these AR genes evolved by duplication events just before the origin of the jawed vertebrates. Our computational analyses suggest that the differences between the three α_1-AR subtypes may affect their tissue specificity, ligand specificity, and possibly signal transduction processes and desensitization. We also show that, within each subtype, differences exist between fish and mammalian receptors, both at the transcriptional and at the physiological level. These differences, however, suggest that the role of α_1-ARs in fish is more complex than previously thought. Our integrated analysis of the α_1-AR gene family suggests that these receptors evolved these distinct features very early within vertebrates.

positive selection; blood pressure; duplication events; fish; gene family

α_1-ADRENOCEPTORS (α_1-ARs) are members of the superfamily of seven transmembrane domain (TMD) receptors coupled to G proteins that mediate the cellular effects of the endogenous catecholamines epinephrine and norepinephrine. The α_1-AR signal transduction pathway is well characterized in mammals (29, 43). Although the precise physiological role and regulation of this heterogeneous group of α_1-ARs remain under intense investigation (8), α_1-ARs are known to be involved with smooth muscle contraction and growth of vascular smooth muscle (29). Although significant species differences exist (32), generally, in mammals, the α_{1A}- and α_{1D}-ARs are expressed in resistance vessels, and both are believed to be involved in the regulation of arterial blood pressure (30, 34). The α_{1B}-AR plays only a minor role in vascular contraction, suggesting that the other subtypes (A and D) are the more important controllers of blood pressure (9).

Our knowledge of α_1-ARs in nonmammalian systems is fragmentary, limited to a few tissues such as liver in some fish species (e.g., Ref. 10) or avian melanocytes (14). These studies are based solely on pharmacology and do not always provide a clear functional delineation of the AR types or subtypes because of the absence of highly selective agonists and antagonists (43). Functional studies of putative α_1-ARs from nonmammalian systems are scarce (41), although recently we demonstrated decreased adrenergic responsiveness in the systemic vasculature of salt-loaded rainbow trout (*Oncorhynchus mykiss*), consistent with desensitization or loss of functional α_1-ARs (7).

Here, we elucidate the evolution of the α_1-AR gene family and study the potential role of these family members in the regulation of blood pressure in a fish model system: the rainbow trout. On the basis of phylogenetic, physiological, and pharmacological evidence, we show that positive selection played a role in the differences between the three subtypes of the α_1-AR family, and that differences exist in the tissue expression profiles of the α_1-AR subtypes and their possible physiological importance between mammals and fish.

MATERIALS AND METHODS

Animals

Rainbow trout (*O. mykiss*) weighing 450–900 g were obtained from Linwood Acres Trout Farm (Campellcroft, ON, Canada). Fish were transported to the University of Ottawa Aquatic Care Facility and were maintained in fiberglass holding tanks (1,275 liters) supplied with well-aerated, dechloraminated City of Ottawa tap water at 13.0°C. Fish were subjected to a constant 12:12-h light-dark photoperiod and fed five times a week with commercial trout pellets [Martin Mills 5 PT, 5 mm in size; composed of 41.0% crude protein (minimum), 11.0% crude fat (minimum), 3.5% crude fiber (maximum), 1.0% calcium (actual), 0.85% phosphorus (actual), 0.45% sodium (actual), 6,800 IU/kg vitamin A (minimum), 2,100 IU/kg vitamin D (minimum), 80 IU/kg vitamin E (minimum), 200 IU/kg vitamin C (minimum)]. Receptor molecular biology was conducted between August and October. Blood pressure experiments were undertaken between August and September. All procedures used were approved by the University of Ottawa Protocol Review Committee and followed standard Canadian Council on Animal Care guidelines on the use of animals in research.

Molecular Procedures

Isolation of tissue RNA. Total RNA was isolated from fresh tissues [brain, efferent branchial artery (EBA), afferent branchial artery (ABA), celiacomesenteric artery (CMA), ventral aorta (VA), dorsal aorta (DA), spleen, liver, kidney, gill, white muscle (WM), posterior cardinal vein (PCV), heart, bulbus arteriosus (BA), intestine] of rainbow trout using TRIzol reagent (Gibco BRL, Burlington, ON, Canada) according to the manufacturer's protocol with the following exception. Four microliters of linear acrylamide (2 mg/μl) (Ambion, Austin, TX) were added after the addition of isopropanol according to the method of Gaillard and Strauss (17) to increase the RNA yield from tissues of small size (EBA, ABA, CMA, VA, and DA). RNA

Article published online before print. See web site for date of publication (http://physiolgenomics.physiology.org).

Address for reprint requests and other correspondence: T. W. Moon, Dept. of Biology, Univ. of Ottawa, Ottawa, ON, Canada K1N 6N5 (e-mail: tmoon@uottawa.ca).

1094-8341/07 $8.00 Copyright © 2007 the American Physiological Society

Downloaded from physiolgenomics.physiology.org on January 7, 2008

concentrations and quality were verified using spectrophotometry (optical density at 260 nm) and RNA gel electrophoresis, respectively.

Amplification of rainbow trout α_1-AR cDNA. An initial set of rainbow trout α_1-AR clones spanning the fourth to the sixth TMD (~350 bp) was amplified using routine RT-PCR strategies. For RT-PCR, cDNA was synthesized using random primers with a First Strand cDNA Synthesis Kit (Roche Molecular Biologicals, Laval, QC, Canada). A preliminary round of PCR amplification was performed using degenerate primers (DP) forward and reverse (DPFR), designed using the CODEHOP program (http://blocks.fhcrc.org/codehop.html) for α_{1A}- and α_{1D}-ARs, and degenerate primers α_{1B}DPF and DPR2 for α_{1B}-AR (Table 1). These degenerate primers were designed based on sequences from the fourth to sixth TMD of rat and human α_1-ARs (GenBank accession nos.: for human α_{1A}-ARs, NP_150646; α_{1B}-ARs, P35368; α_{1D}-ARs, NP_000669; for rat α_{1A}-ARs, NP_058887; α_{1B}-ARs, AAA63478; α_{1D}-ARs, P23944). Subsequently, because the sequence of TMD7 was required to design real-time PCR primers (a proposed intron is located between TMD6 and TMD7; see below), another 3′-degenerate primer (DPR2) was designed for the α_{1A}-, α_{1B}-, and α_{1D}-ARs (Table 1) based on the previous alignment. In addition, an α_{1D}-AR 5′-degenerate primer (α_{1D} DPF) designed on the basis of the sequence alignment of TMD1 of human and rat α_{1D}-ARs amplified TMD1 to TMD7 of the trout α_{1D}-AR once paired with the α_{1D}-DPF and DPR2 degenerate primers. Trout clones were sequenced (Ottawa Genome Centre), and gene-specific primers (GSPs) were designed (Primer 3 program; http://frodo.wi.mit.edu/cgi-bin/primer3/primer3_www_slow.cgi) from these sequences for 5′ and 3′ rapid amplification of cDNA ends (RACE).

RACE PCR for α_{1A}- and α_{1D}-AR. The 5′- and 3′-RACE system for rapid amplification of cDNA ends (version 2, Gibco BRL) was used to amplify the 5′- and 3′-ends of the trout α_1-AR cDNA. α_{1A}-AR 5′-end sequences were obtained through 5′-RACE using trout α_{1A}-AR GSP1 (Table 1) to prime cDNA synthesis. This cDNA was then used as the template in an initial round of PCR amplification using a second trout α_{1A}-AR GSP2 (Table 1) and the 5′-amplification primer provided with the kit. A 5-μl aliquot of this initial PCR amplification step was then used as a template for a second round of nested PCR using a third trout α_{1A}-AR GSP3 (Table 1) and the abridged universal amplification primer (AUAP) provided with the kit. α_{1D}-AR 5′-RACE was performed using the same procedure as for the α_{1A}-AR using α_{1D}-GSPs. Synthesis of cDNA for α_{1A}-AR 3′-RACE was performed by priming with the 3′-amplification primer provided in the kit. A first round of PCR amplification was performed using trout α_{1A}-AR GSP4 (Table 1) and AUAP. A second round of semi-nested PCR amplification using trout α_{1A}-AR GSP5 (Table 1) and AUAP was then carried out. α_{1D}-AR 3′-RACE was performed using the same procedure as noted for the α_{1A}-AR using α_{1D}-GSPs. The PCR products were cloned using the TOPO TA cloning kit (Invitrogen, Burlington, ON, Canada). To confirm sequence accuracy, all three α_1-AR subtype genes were cloned three times using different PCR reactions, and each clone was sequenced on both strands (Ottawa Genome Centre). All PCR amplifications described above used the following regimen of denaturing, annealing, and extension: 1× 2 min at 94°C, 35× (30 s at 94°C, 30 s at 55°C, 1 min at 72°C), and 1× 10 min at 72°C; annealing temperature was 55°C (Table 1). All primers were ordered from Invitrogen.

Gene cloning of α_{1B}-AR. Using degenerate α_{1B}DPF and DPR2, a partial α_{1B}-AR sequence was obtained of 462 bp. A full-length α_{1B}-AR gene was obtained by using this sequence and "mining" the cGRASP expressed sequence tag (EST) clustering (http://web.uvic.ca/cbr/grasp) database to add 5′- and 3′-sequence. With the use of GSPs (α_{1B}-GSP1 and α_{1B}-GSP2 for the fragment from the 5′-end to TMD6; α_{1B}-GSP3 and α_{1B}-GSP4 for the fragment from TMD5 to the 3′-end) (Table 1), a full-length sequence was cloned. The PCR, cloning, and sequencing procedures were as described above.

Real-time PCR analysis of α_1-AR genes: tissue distribution. α_1-ARs (α_{1A}, α_{1B}, and α_{1D}) and β-actin (internal control) were assessed using real-time PCR analysis (Stratagene MX-4000), and DNA amplification was performed using SYBR Green (Molecular Probes, Eugene, OR) according to the manufacturer's protocol. PCR primers were designed that spanned the hypothetical intron-exon boundary within TMD6 and TMD7 to avoid genomic DNA amplification (1, 43). The real-time PCR primers (Table 1; QP) were designed and synthesized to yield 170- to 200-bp amplicons (α_{1A}-AR, α_{1D}-AR, and β-actin, 170 bp; α_{1B}-AR, 200 bp). The real-time PCR products were cloned to ensure that the amplification was identical to the original sequence. Forty cycles of a two-step PCR protocol were used: 1× 15 min at 95°C, 40× (30 s at 95°C, 30 s at 58°C, 30 s at 72°C), and 1×

Table 1. *Primers designed to amplify various sequences of trout α_1-ARs and primers designed for real-time PCR*

	5′ Forward Primers	3′ Reverse Primers	T_m, °C
DPFR	GGITGGMRISARCCIGCICCIRAIGAYGA	CTYTTIGCIGCYTTYTTYTCICK	55
DPR2		TGGGGTTGATGCAGGAGTTNARRTANCC	55
α_{1A}GSP1		CATAGGCAGGCTCCTCTGTG	55
α_{1A}GSP2		TAGTGTGTGACTGTTCGTAG	55
α_{1A}GSP3		ATTGTCCCAAGTATCAGTCC	55
α_{1A}GSP4	GACAAGTCAGACTCAGAGAGCAT		55
α_{1A}GSP5	CCTGCGCCTCCTCAAGTTCT		55
α_{1B}DPF	CAAAGAGTGCGGCATCACCSARRARCCNTT		55
α_{1B}GSP1	GGGATGGTGTTGCTTGTTTT		55
α_{1B}GSP2		GCGGAAGTCTGGATTGAAAG	55
α_{1B}GSP3	GGTTGGCATGTTTACGCTTT		55
α_{1B}GSP4		CACCTTATCCTCAGGTATGT	55
α_{1D}DPF	TGTCCGCCCAGGGCRTNGGNGTNGG		55
α_{1D}GSP1		CGGTAGCCAACACAGGATGA	55
α_{1D}GSP2		TTTTGGCAGCCTTCTTCTCC	55
α_{1D}GSP3		GCATGCTCCGACAGTGAATC	55
α_{1D}GSP4	CCCTCTTCTCCTCGCTCTTT		55
α_{1D}GSP5	GCACTGAAGCCATCTGACAT		55
α_{1A}QPFR	CTGCGCCTCCTCAAGTTCTC	CCCCAGCCAGAAGGTGATCT	58
α_{1B}QPFR	TCTCAGGTGCAGGATGACAG	GCGGAAGTCTGGATTGAAAG	58
α_{1D}QPFR	CTGTCCGTGCGCTTGATGAA	AACCCAGCCAGAAGATGACC	58
β-actinFR	CGTCCCAGGCATCAGGGAGT	TCTCCATGTCGTCCCAGTTG	58

Gene-specific primers (GSPs) were designed online using the program Primer 3, and degenerate primers (DP) were designed using the CODEHOP program. T_m is the annealing temperature used in the PCR amplification. DPF, degenerate primer forward; DPR, degenerate primer reverse; QP, real-time PCR primer.

Downloaded from physiolgenomics.physiology.org on January 7, 2008

10 min at 72°C. A no template control for each master mix and a no reverse transcriptase control were included in each analysis. The slopes of the standard curves for α_{1A}-AR, α_{1B}-AR, α_{1D}-AR, and β-actin were −3.083, −3.002, −3.003, and −3.015, respectively, yielding amplification efficiencies of 111, 115.3, 115, and 114.6%. Real-time PCR data are reported using the comparative ΔCt method (Ct is threshold cycle) described by Livak and Schmittgen (23) and are given by the following formula: $2^{(-\Delta\Delta Ct)}$, where $\Delta\Delta Ct = [(Ct_{\alpha 1\text{-AR}} - Ct_{\beta\text{-actin}}) - (Ct_{\alpha 1\text{-AR}} - Ct_{\beta\text{-actin}})x]$; $(Ct_{\alpha 1\text{-AR}} - Ct_{\beta\text{-actin}})x$ represents the ΔCt for the tissue expressing the highest value of $(Ct_{\alpha 1\text{-AR}} - Ct_{\beta\text{-actin}})$ for that particular α_1-AR subtype. A Ct is defined as that point where fluorescence level exceeds the baseline.

Phylogenetic analysis and prediction of phosphorylation sites. Rainbow trout α_1-AR amino acid sequence homologs from selected chordate genomes were searched in GenBank using reciprocal best basic local alignment search tool (BLAST) hits (22). As of June 2007, no homolog could be found in the draft of the *Ciona* genome using either tBLASTx or PSI-BLAST, the two most sensitive flavors of BLAST. The sequences found are listed in Table 2. The out-group sequences are based on the dopamine D1 receptor, as first, it is the closest relative to the α_1-AR in a phylogenetic study (16), and second, the dopamine receptor appeared as the best reciprocal BLAST hit of α_1-ARs in lower vertebrates. Sequences were aligned with CLUSTAL W version 1.8 (35) at the amino acid level and back translated to DNA to obtain the nucleotide sequence alignments. Alignments were checked and adjusted by eye where necessary and are available on request. The sequence segment used for phylogenetic analyses spanned from the conserved amino end of TMD1 to the end of the conserved carboxyl end of TMD7. To check for consistency among different substitution and analysis models, phylogenetic analyses were conducted in a Bayesian framework with MrBayes 3.1.2 (31) at two levels: amino acids and codons. At the amino acid level, we constructed a reversible-jump Markov chain Monte Carlo (RJ-MCMC) that integrates over 10 empirical models of protein evolution (21, 31). This approach circumvents the issue of model selection, as it does not rely on one single model of evolution, sampling phylogenetic trees in proportion to their posterior probability. We also obtained Bayesian estimates under a codon substitution model (19). For both types of data, we used a discrete Γ distribution with five rate categories (38) plus an invariable class of sites. Under each model, four independent RJ-MCMC samplers were run for 5×10^6 steps each. Standard tempering procedures were used to improve mixing, with each sampler consisting of four chains, three of which heated to different temperatures (e.g., Ref. 31). Steps along the chain were sampled every 10^4 accepted steps to decrease autocorrelation among the samples. The 10^5 first accepted steps were discarded from each chain ("burn-in"). Functional divergence was tested using PAML version 3.15 (38) as described in Ref. 5. The sites potentially under positive selection during the period of duplication events were identified using a "branch site" model (39) with the "test of positive selection" described in Ref. 42. Briefly, this test compares two models to assess whether the presence of sites under positive selection is statistically significant in a branch of interest, the "foreground" branch (e.g., branch with rate ratio ω_1 in Fig. 4). This model, referred to as H_2^A hereafter, has four categories of sites: *category 0* includes conserved codons, with $0 < \omega_1^{(0)} < 1$ estimated from the data; *category 1* includes codons that evolve neutrally $[\omega_1^{(1)} = 1]$; *categories 2a* and *2b* include codons that are conserved or neutral in the background branches but are under positive selection in the foreground branch, with $\omega_1^{(2)} > 1$ estimated from the data. This model introduces four free parameters. The test of positive selection compares this model against a simpler model, H_2^{A0}, that does not allow for positive selection [$\omega_1^{(2)}$ is set to 1]. This latter model has three free parameters. To be conservative, we used χ_1^2 to approximate the distribution of the test statistic under the null hypothesis that there is no difference between models H_2^A and H_2^{A0} (42). Sites positively selected in the test of positive selection were identified by the Bayes empirical Bayes (BEB) procedure (40), which improves on the naive empirical Bayes approach (NEB; Ref. 27) by accommodating uncertainties of the maximum likelihood estimates. Four sets of foreground branches were tested: in "*test 1*," these are the four branches right after the two duplication events; in "*test 2*," it is the branch that precedes the two duplication events; in "*test 3*," these are the two branches after the first duplication event leading to paralogs A and B+D; and in "*test 4*," these are the two branches after the second duplication event leading to paralogs B and D. A Bonferroni procedure was used to correct for multiple tests. To check for convergence of the maximum likelihood optimization procedures, all the analyses were run four times starting from different parameter values. The software NETPHOS 2.0 (http://www.cbs.dtu.dk/services/NetPhos/) was used to predict the phosphorylation sites in the third intracellular loop and COOH-terminal region of the rainbow trout α_1-AR sequences. Three-dimensional (3D) structure predictions were performed by homology modeling with SWISS-MODEL (2) and 3D-JIGSAW (4), based on the human D paralog (accession no.: NP_000669). Both tools predict structures by first aligning a query (protein sequence) or some of its parts to one or more template protein

Table 2. *GenBank accession nos. of sequences used for the generation of phylogenies noted on Fig. 4*

	α_{1A}-AR	α_{1B}-AR	α_{1D}-AR
Human	NP_150646	P35368	NP_000669
Chimpanzee ("pan")	XP_525254		
Rhesus monkey ("macaca")	XP_001108664	XP_001083528	
Rat	NP_058887	AAA63478	P23944
Mouse	P97718	CAA73272	P97714
Rabbit	O02824	AAF80280	O02666
Pig	CAB62570	CAE46112	CAB59347
Dog	O77621	P11615	
Cow	P18130		
Guinea pig	AAD22540	AAD22542	AAD22541
Golden hamster		P18841	
Opossum ("monodelphis")	XP_001380260	XP_001369817	
Gallus gallus ("chicken")	XP_425762	XP_414483	XP_420871
Medaka	Q91175		
Puffer fish	http://www.ncbi.nlm.nih.gov/BLAST/Genome/fugu.html		
Zebrafish	http://www.ncbi.nlm.nih.gov/genome/seq/DrBlast.html		
Amphioxus		CAA06536	
Florida lancelet dopamine D1 receptor		AAQ91625	
Atlantic hagfish dopamine D1 receptor		CAA06542	

Names in parentheses refer to nomenclature in Fig. 4.

Downloaded from physiolgenomics.physiology.org on January 7, 2008

sequences, as determined by BLASTp searches; these templates must have a resolved 3D structure deposited in the Protein Data Bank (http://www.pdb.org/pdb/home/home.do). These 3D segments are stitched together to form a preliminary model. The model is then examined for potential collisions between atoms and is finally refined by limited energy minimization.

Physiological Procedures

Blood vessel cannulation. Trout were fitted with a dorsal aortic cannula (33) to monitor blood pressure. Trout were anesthetized by immersion in a cold oxygenated benzocaine solution (0.1 g/l) until voluntary activity ceased. A single indwelling cannula (Clay-Adams PE50 polyethylene tubing) was placed into the dorsal aorta at the level of the first gill arch while the same anesthetic solution was passed continuously across the gills. The cannula was sutured to the roof of the mouth and filled with heparinized saline (100 IU/ml sodium heparin); dorsal aorta pressure (P_{DA}) was monitored through this cannula using a UFI model 1050BP (UFI, Morro Bay, CA) pressure transducer calibrated using a water column. The P_{DA} signal was recorded with a data acquisition system (Biopac System, Goleta, CA) and collected using Acknowledge 3.03 (Biopac System) data acquisition software; sampling frequency was 10 Hz. Systemic resistance (R_S) was calculated as mean P_{DA}/V_b (cardiac output). When drugs were administered, the caudal vein also was cannulated in the anterior direction following exposure of the hemal arch by a lateral incision (~2 cm long) at the level of caudal peduncle (see Ref. 3). Cardiac output was monitored with a 3S ultrasonic flow probe (Transonic Systems, Ithaca, NY) placed around the bulbus arteriosus, which was exposed by a small (~1.5 cm) ventral midline incision to expose the pericardium. Lubricating jelly (K-Y Personal Lubricant, Johnson and Johnson) was used as an acoustic couplant. The incisions were closed, and the caudal cannula and flow probes were anchored to the skin using silk sutures. The tubing and cannulas were flushed with cold heparinized saline, and trout were revived by flushing the gills with aerated water until opercular movements became pronounced and regular. Following surgery, fish were placed into individual opaque acrylic chambers supplied with aerated, flowing aquaria water (flow rate >2.5 l/min). The fish were allowed to recover for 24 h before experiments were initiated. The chambers were small

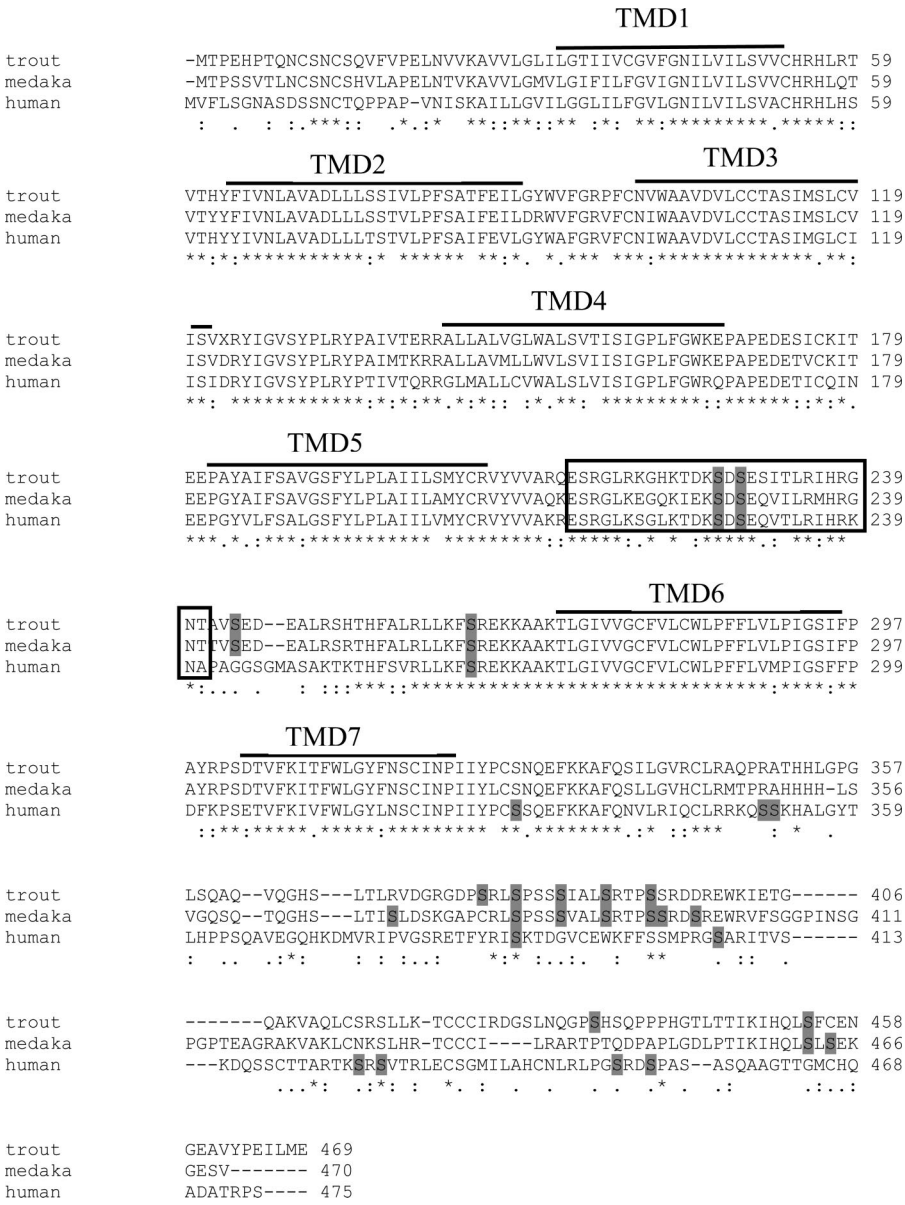

Fig. 1. Alignment of the rainbow trout α_{1A}-adrenoceptor (AR) amino acid sequence with human (NP_150646) and medaka (Q91175) α_{1A}-ARs. Asterisk (*) indicates identical sequences, colon (:) indicates fully conserved "strong groups," and period (.) indicates fully conserved "weak groups," as identified by CLUSTAL W. Transmembrane domains (TMDs) are shown as a heavy line, and the G protein binding domain is indicated by a box; highlighted serine residues are potential protein kinase A-, protein kinase C-, or G protein-coupled receptor kinase phosphorylation sites, as defined by NETPHOS 2.0.

Downloaded from physiolgenomics.physiology.org on January 7, 2008

enough to prevent the fish from turning or rolling but did not interfere with ventilation or tail movements. After the fish were placed into the boxes, the room was darkened until completion of the experiment.

α_{1A}- and α_{1D}-AR selective antagonists: in vivo injection and drugs. The mammalian selective α_{1A}-AR antagonist RS-17053 and α_{1D}-AR antagonist BMY-7378 were purchased from Tocris Cookson (Ellisville, MO). BMY-7378 was dissolved in distilled water to a stock concentration of 100 mM and then diluted in 0.9% saline to the required working concentrations. RS-17053 was prepared in DMSO to a stock concentration of 100 mM and then diluted in distilled water; final DMSO concentrations did not exceed 1%. To maintain normal osmolarity, mannitol was added to the working RS-17053 solutions. Control injections included 0.9% saline for BMY-7378 and DMSO plus mannitol for the RS-17053 experiments. Drug (0.6 ml/kg) was delivered slowly through the caudal vein cannula over a 45- to 60-s interval. A preliminary series of experiments injected six different drug doses (0.001, 0.01, 0.1, 0.5, 1, and 2.5 mg/900 g fish) from the lowest to the highest dose; each dose was given to each fish, but the next dose was injected only after all cardiovascular variables had stabilized. This provided a dose-response curve for the particular drug; however, a drug dose of 2.5 mg was found to be lethal to the trout. With the use of R_S as an index, the drug dose that decreased R_S by 70% of the control was used to determine the effects of catecholamine injection on cardiovascular parameters; this dose was 0.5 and 1 mg for RS-17053 and BMY-7378, respectively.

A catecholamine cocktail (2.5×10^{-5} M; see Ref. 7) was injected (0.6 ml/kg) into a fish through the caudal vein cannula; after cardiovascular parameters had stabilized, one of the antagonists was then injected. Following stabilization of the cardiovascular variables, another dose of the catecholamine cocktail (0.6 ml/kg) was injected into the cannula to determine sensitivity following antagonist application. Peak responses and plateau responses were determined for each parameter after injection.

RESULTS

Sequence Analysis

Three full-length α_1-AR sequences were cloned from trout: the α_{1A}-AR sequence (GenBank accession no.: DQ278449) encodes a 478-amino acid protein (Fig. 1), the α_{1B}-AR sequence (GenBank accession no.: EF667964) encodes a 511-amino acid protein (Fig. 2), and the α_{1D}-AR sequence (GenBank accession no.: DQ177150) encodes a 514-amino acid protein (Fig. 3). Each sequence exhibits the characteristic seven TMD structure of their mammalian AR homologs. As with other fish ARs (26), alignment of the three rainbow trout α_1-AR subtypes with α_1-AR sequences from various vertebrate species shows the greatest residue conservation within the TMDs, whereas the greatest diversity is found at the NH_2- and COOH-terminal regions. Amino acid identities between these

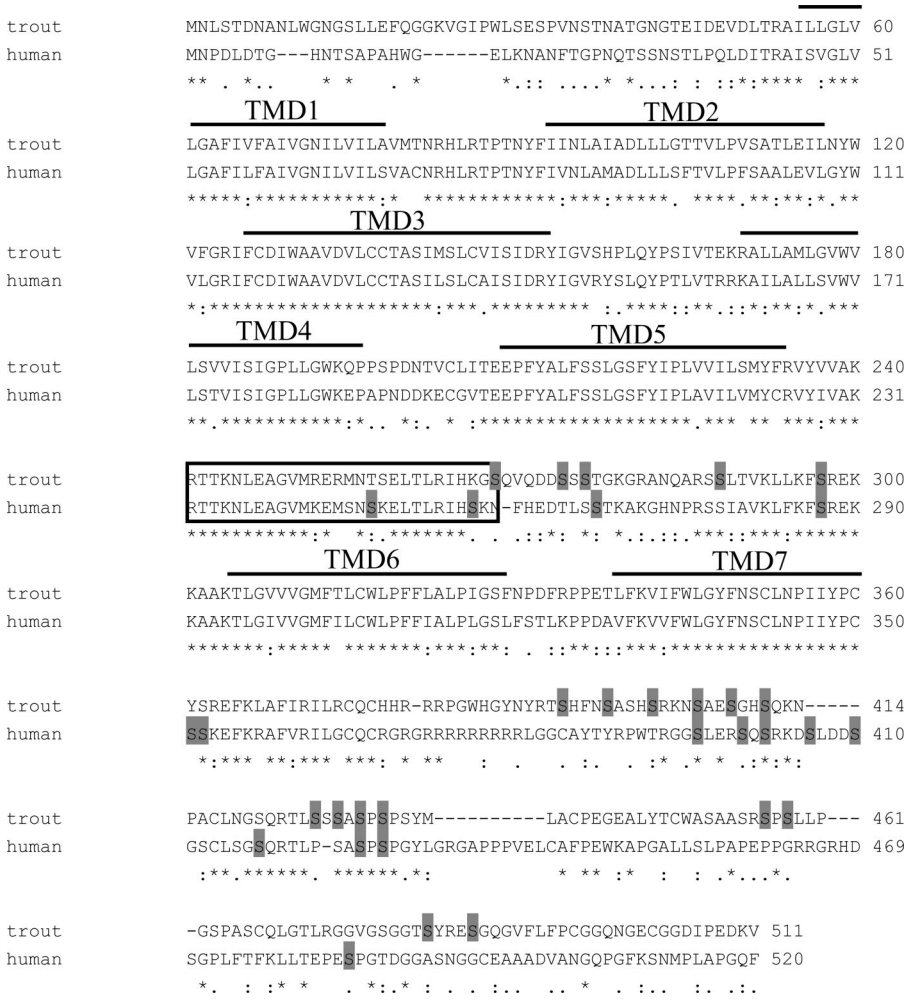

Fig. 2. Alignment of the rainbow trout α_{1B}-AR amino acid sequence with human (P35368) α_{1B}-ARs. See legend to Fig. 1 for further details.

Downloaded from physiolgenomics.physiology.org on January 7, 2008

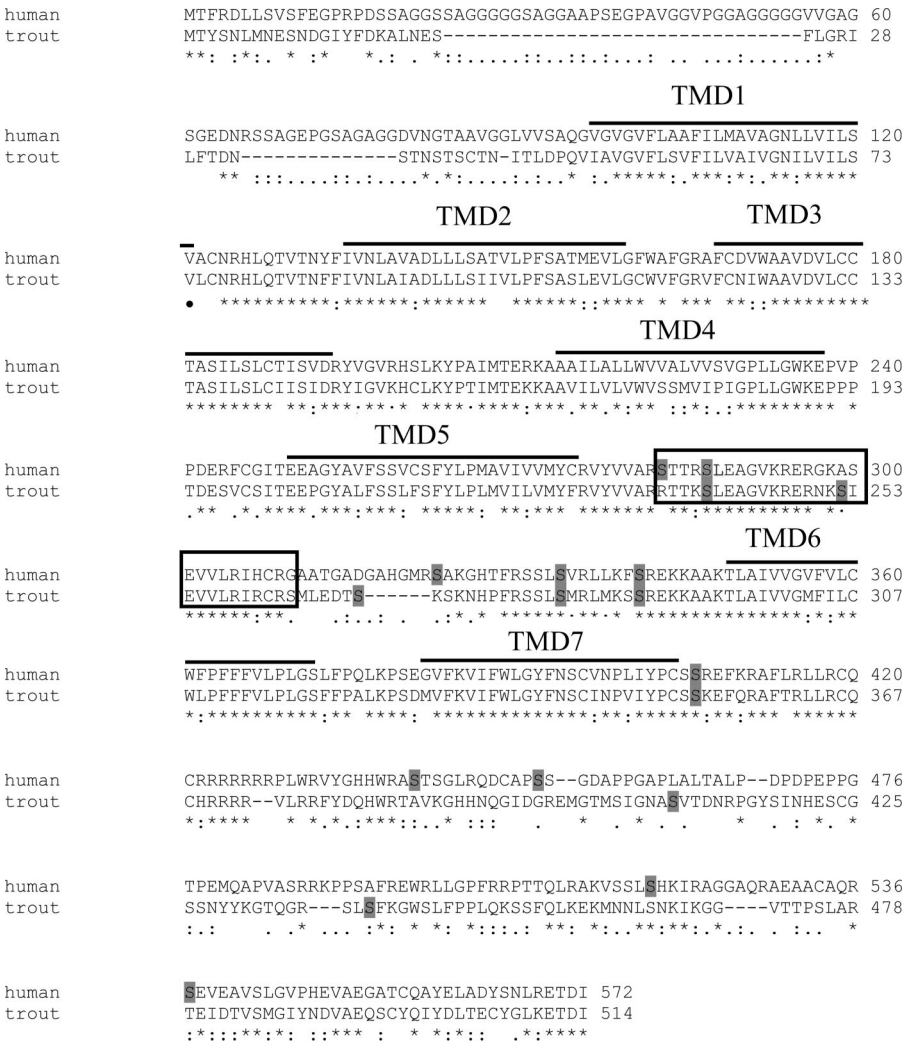

Fig. 3. Alignment of the rainbow trout α_{1D}-AR amino acid sequence with human α_{1D}-AR (NP_000669). See legend to Fig. 1 for further details.

trout α_1-ARs and their homologs deposited in GenBank (Table 2) range between 56 and 89%.

Computational Analyses

Bayesian analyses at the amino acid and codon levels consistently produced a tree comprising three major clades: α_{1A}-ARs, α_{1B}-ARs, and α_{1D}-ARs (Fig. 4), all supported by posterior probabilities >0.95. The amino acid (Fig. 4*A*) and codon (Fig. 4*B*) tree topologies are slightly different, but both present a consistent picture. Although the sequences chosen as out-groups are very divergent, our large data sets both place the root of the tree at the same location: our results suggest that α_{1A}-ARs were the first to split, followed by α_{1D}- and α_{1B}-ARs (Fig. 4). Incidentally, two of the α_{1A}-AR sequences retrieved from GenBank are likely to be misannotated (Fig. 4): the predicted opossum (XP_001380260, encoded by XM_001380223) and the predicted chimpanzee (XP_525254, encoded by XM_525254) ARs. Both sequences seem to belong to the α_{1D}-AR clade with high probabilities.

Both the amino acid (Fig. 4*A*) and the codon (Fig. 4*B*) trees were then used to test whether the duplication events could have led to functional divergence. To this effect, we specified nested codon substitution models (Fig. 4; Table 3), where selective pressures were measured by estimating the nonsynonymous-to-synonymous rate ratio. This ratio is denoted ω, with $\omega = 1$, <1, and >1, indicating neutral evolution, negative or positive selection, respectively. The statistical approach used to detect functional divergence (5) allowed us to reject the null hypothesis (H_0) of a constant selective regime in favor of the alternative H_5, which allowed different selective regimes during and after the duplication events (Table 3). The results, presented in Table 3, show that the amino acid and the codon trees virtually give the same results and suggest the presence of a strong signal for positive selection along the four branches right after the two duplication events ($\omega_1 = \infty$; $P < 2.0 \times 10^{-12}$). However, when testing for the existence of sites under positive selection in these exact four branches (*test 1* in Table 4), no significant signal was detected with either the amino acid tree or the codon tree ($P = 0.7083$; Table 4). One potential explanation of these conflicting results is that distinct episodes of positive selection affected different sets of sites. These distinct episodes would most likely have resulted from the two duplication events leading to paralogs α_{1A}, α_{1B}, and α_{1D}. To test this hypothesis, we specifically designed *tests 2–4* (Table 4). Our *test 2* shows that there is no evidence for positive selection before the duplication events, while *test 3* and *test 4* show that both duplication events were followed by episodes of

Downloaded from physiolgenomics.physiology.org on January 7, 2008

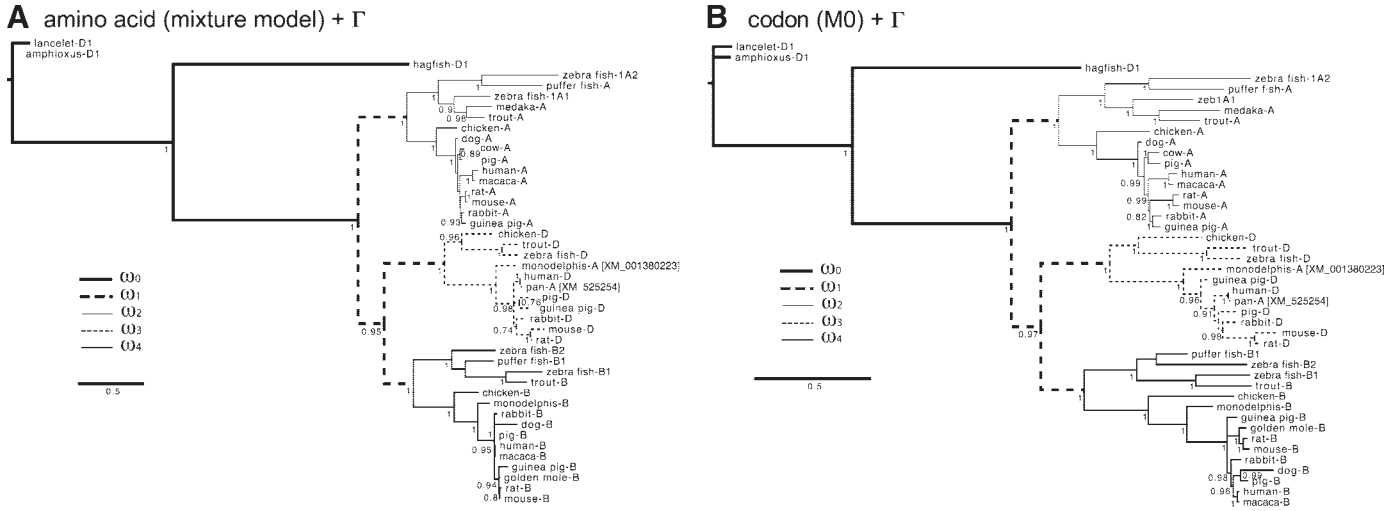

Fig. 4. Bayesian estimates of the phylogeny of the AR gene family and model specifications for testing for positive selection. Two substitution models were used. *A*: reversible-jump Markov chain Monte Carlo results over amino acid substitution models + Γ_5. *B*: codon substitution model + Γ_5. Posterior probabilities indicated when >70%.

positive selection. The results presented in Table 4 also show that, while the signal for positive selection during these two episodes is significant at the 5% level (after Bonferroni correction), there exists some variation in the confidence we can have in the exact identity of the sites identified by the BEB procedure. The identity of the sites found after the first duplication event with *test 3* seems to be robust to the tree topology, as exactly the same sites are found under the amino acid tree and the codon tree. However, the identity of the sites found after the second duplication event with *test 4* is not so robust to the specification of the tree topology: only site 531A shows a consistent signal. It is also apparent from Table 4 that, with the possible exception of site 284T, the two episodes of positive selection affected different sites, as we first hypothesized. Taken together, these results suggest that two episodes of functional divergence occurred just after the duplication events, and that each episode affected different sites.

Several putative serine phosphorylation sites were inferred in each sequence within the third intracellular loop and COOH-terminal tail (Figs. 1–3). The putative phosphorylation sites are generally not shared among subtypes, and their numbers also vary among subtypes. The putative phosphorylation sites identified here are also distinct from the sites putatively involved in the functional divergence of the three AR types, except for site 284T (see above). As of July 2007, no 3D structures for ARs were deposited in the Protein Data Bank (PDB; http://www.pdb.org), and BLASTp similarity searches using the protein sequence of the human α_{1D}-AR failed to return any structure from PDB. Homology modeling with SWISS-MODEL (2) produced only a short structural model between residues 93 and 288, based on the low-resolution (4.15Å) template whose PDB ID is 2i37 (photoactivated rhodopsin). 3D-JIGSAW (4) produced a larger model that mostly encompassed the previous template. This model spanned positions 93-413 (Fig. 5). Note that 3D-JIGSAW is more liberal than SWISS-MODEL, so that our structural model is expected to be somewhat inaccurate. Despite this, seven α-helices were predicted (Fig. 5); these likely correspond to the seven TMDs of the AR. Note that most of the sites putatively evolving under positive selection belong to transmembrane domains or to cytoloop-3, with the possible exception of site 241P (Fig. 5). Cytoloop-3 contains a G protein binding domain that functionally differentiates AR types and subtypes (8).

AR Subtype mRNA Tissue Distribution

Real-time PCR was used to analyze α_{1D}-, α_{1A}-, and α_{1B}-AR gene expression in 15 trout tissues. β-Actin was selected as a reference gene, as it showed stable expression; the difference between the highest and lowest expression among the 15 tissues sampled was two cycles. A unique probe of 20 bases was designed for each α_1-AR subtype corresponding to the region that displayed the greatest variation among the three subtypes as determined by the multiple alignments of α_{1D}-, α_{1A}-, and α_{1B}-AR gene sequences. Most tissues examined contained all three α_1-AR transcripts (Fig. 6), including pe-

Table 3. *Model comparisons and parameter estimates under models of constant (H_0) or variable ω rate ratios across clades (H_5)*

Tree	Model	l	No. of Parameters	*P* Value	Parameter Estimates
AA	H_0	−34,635.72	1	NA	$\omega_0 = 0.0772$
	H_5	−34,605.33	5	2.0×10^{-12}	$\omega_0 = 0.1097$; $\omega_1 = \infty$; $\omega_2 = 0.0704$; $\omega_3 = 0.0901$; $\omega_4 = 0.0720$
Codon	H_0	−34,587.28	1	NA	$\omega_0 = 0.0792$
	H_5	−34,555.91	5	7.7×10^{-13}	$\omega_0 = 0.1096$; $\omega_1 = \infty$; $\omega_2 = 0.0708$; $\omega_3 = 0.0914$; $\omega_4 = 0.0774$

AA, amino acid tree (Fig. 4*A*); Codon, codon tree (Fig. 4*B*); l, log-likelihood value; NA, not applicable. Compared models: H_0, $\omega_0 = \omega_1 = \omega_2 = \omega_3 = \omega_4$; H_5, $\omega_0 \neq \omega_1 \neq \omega_2 \neq \omega_3 \neq \omega_4$.

Downloaded from physiolgenomics.physiology.org on January 7, 2008

Table 4. *Branch site tests of positive selection*

Tree	H_2	*Test 1*	*Test 2*	*Test 3*	*Test 4*
AA	H_2^{A0}	−33,902.08	−33,920.74	−33,909.75	−33,919.25
	H_2^{A}	−33,902.01	−33,918.22	−33,903.849038	−33,915.11
	P	0.7083	0.0248	0.0006	0.0040
	Sites	NS	NS	110A, 132N, 259S, 284T, 293V, 332S, 356V, 407R, 415R, 418C, 434Y	241P, 253G, 284T, 329F, 531A
Codon	H_2^{A0}	−33,854.88	−33,872.46	−33,862.41	−33,871.83
	H_2^{A}	−33,854.81	−33,870.04	−33,857.35	−33,867.75
	P	0.7083	0.0278	0.0015	0.0043
	Sites	NS	NS	110A, 132N, 259S, 284T, 293V, 332S, 356V, 407R, 415R, 418C, 434Y	253G

The foreground branches are specified as follows in each test. *Test 1*: the 4 branches right after the 2 duplication events. *Test 2*: the branch that precedes the 2 duplication events. *Test 3*: the 2 branches after the first duplication event leading to paralogs A and B+D. *Test 4*: the 2 branches after the second duplication event leading to paralogs B and D. *P* values are computed assuming that the test statistic (twice the log-likelihood difference) asymptotically follows a χ_1^2 distribution under the null hypothesis. The 5% significance threshold after Bonferroni correction is at $P = 0.0125$. Positively selected sites were identified by Bayes empirical Bayes at a posterior probability cutoff of 99%; the reference sequence is *Homo sapiens* paralog D (NP-000669).

ripheral arteries, consistent with previous studies in rats and humans (e.g., Ref. 20). In general, the α_{1D}-AR mRNA was highly expressed in the ABA, spleen, VA, brain, and EBA, with highest expression in BA and little expression in the heart (Fig. 6*A*). α_{1A}-AR mRNA expression was relatively high in WM, EBA, DA, VA, gill, and spleen, with highest expression in brain, but was not detectable in the ABA and detected only at low levels in the heart (Fig. 6*B*). However, α_{1B}-AR showed a different expression pattern, with high expression detected in WM, spleen, and PCV and the highest in brain; most arteries examined showed relatively little α_{1B}-AR expression (Fig. 6*C*).

α_{1A}- and α_{1D}-AR Selective Antagonists: In Vivo Injection

The involvement of α_1-ARs in the vascular response of the rainbow trout was confirmed with the use of α_1-AR selective antagonists. The catecholamine cocktail significantly increased blood pressure (BP) and R_S, whereas both the selective α_{1A}- and α_{1D}-AR antagonists RS-17053 and BMY-7378, respectively, at a dose that decreased R_S by 70% of the control significantly decreased these parameters (Table 5). In addition, reinjecting the same catecholamine cocktail following antagonist administration resulted in a rise in both BP and R_S, but this increase was not significantly different from preinjection values. No changes occurred in cardiac output (CO) under these conditions.

DISCUSSION

Functional Divergence of the α_1-AR Gene Family Members

Our computational analyses revealed some important results (Fig. 4). Each of the genes we sequenced from rainbow trout is clearly (with posterior probabilities >0.95) identified as a member of the α_1-AR family: α_{1A}-AR, α_{1B}-AR, or α_{1D}-AR. This means that these are fish homologs of the three mammalian α_1-AR subtypes that are well studied at the molecular,

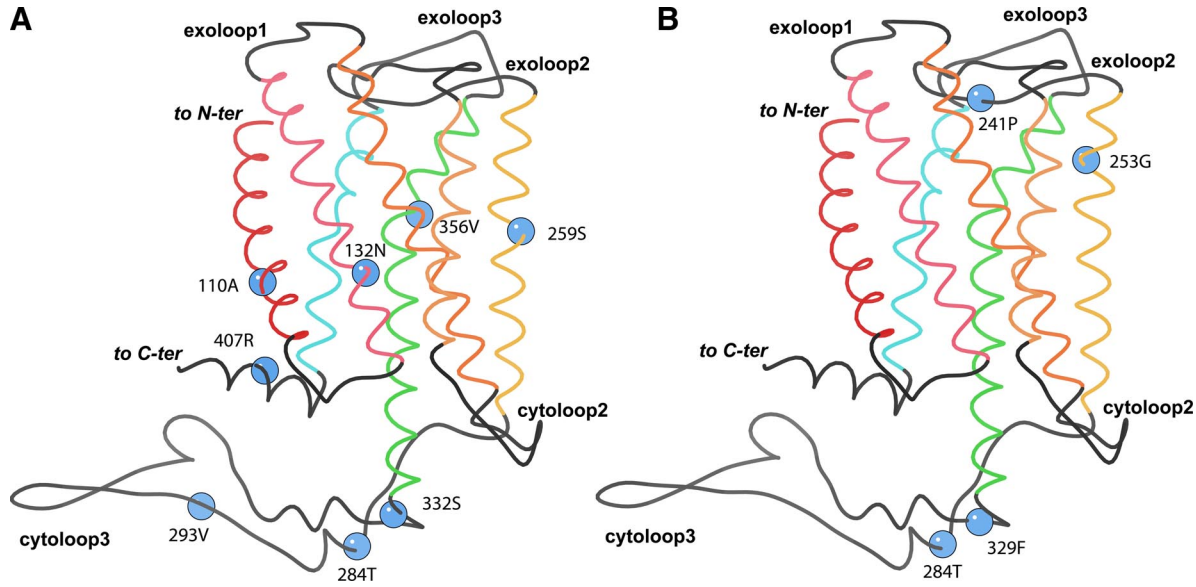

Fig. 5. Three-dimensional model of the human α_{1D}-AR with putatively selected sites. *A*: amino acid sites identified by *test 3* on the two branches after the first duplication event leading to paralogs A and B+D. *B*: sites identified by *test 4* on the two branches after the second duplication event leading to paralogs B and D. Only residues 93–413 were predicted by homology modeling with 3D-JIGSAW. Blue spheres represent the position of the N atom of each site predicted to be under positive selection. N-ter, NH_2 terminus; C-ter, COOH terminus.

Downloaded from physiolgenomics.physiology.org on January 7, 2008

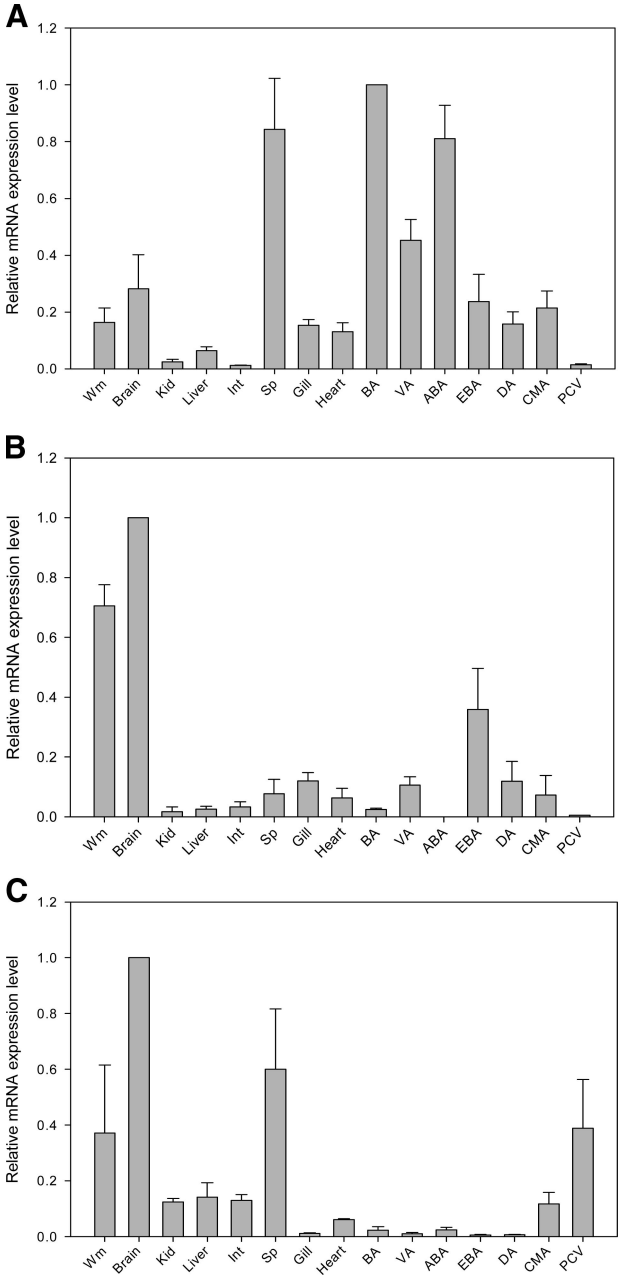

Fig. 6. Real-time PCR analysis showing the tissue distribution of α_{1D}-AR (*A*), α_{1A}-AR (*B*), and α_{1B}-AR (*C*) mRNA in 15 trout tissues. Equal amounts of total RNA were used in cDNA synthesis for real-time PCR. Data are reported as relative mRNA expression level using $2^{(-\Delta\Delta Ct)}$ (see MATERIALS AND METHODS for details); β-actin is used as an internal control gene. All values of a particular α_1-AR subtype are compared with the tissue showing the highest expression level of that α_1-AR subtype ($n = 3$ individual fish). The 15 tissues are as follows: white muscle (WM), whole brain, kidney (Kid), liver, intestine (Int), spleen (Sp), gill, heart, bulbus arteriosus (BA), ventral aorta (VA), afferent branchial artery (ABA), efferent branchial artery (EBA), dorsal aorta (DA), celiacomesenteric artery (CMA), and posterior cardinal vein (PCV).

pharmacological, and physiological levels. The apparent lack of homologs to AR sequences in the draft of the *Ciona* genome and from Hyperotreti (hagfishes) suggests that ARs evolved after the urochordate-chordate split but before the differentiation of jawed vertebrates. Because of this absence of a closely related ortholog in the databases, we used the more diverged dopamine receptor genes from lower vertebrates to root the phylogeny of the AR paralogs. Although distant out-groups are known to create difficulty for phylogenetic analyses (12), our two large data sets at the amino acid (Fig. 4*A*) and codon (Fig. 4*B*) levels suggest a consistent scenario where a first duplication event led to the evolution of α_{1A}-ARs and to proto-α_{1B}-ARs/α_{1D}-ARs; a second duplication event then led to the α_{1B}-ARs and α_{1D}-ARs. This hypothesis should be further assessed by extending sampling to include more taxa.

The persistence of different paralogs might suggest functional diversification among the members of the α_1-AR family. This hypothesis would imply that the selective forces maintaining the ancestor to the α_1-AR members of the gene family relaxed following the duplication events, and that this relaxation permitted a short period of positive selection. We tested specifically for this scenario using a statistical approach (Tables 3 and 4) and showed that the period during which the duplication events occurred is characterized by a burst of positive selection ($\omega = \infty$; $P < 2.0 \times 10^{-12}$). A more detailed analysis showed that each duplication event was followed by independent episodes of positive selection that affected different sites. This potentially forms the basis of the functional differentiation between the three α_1-ARs included in this study. Although the accurate identification of sites under positive selection is difficult (42), our results show that most of these sites either belong to transmembrane domains or to the third cytoloop of the receptor. Our results suggest that the differentiation of these receptors is therefore likely to have involved both the ligand specificity and the type of signal transduction. This is consistent with the known differences between these receptors (e.g., Ref. 8).

Phosphorylation plays a key role in the desensitization, downregulation, and internalization of α_1-ARs (6), and a study of the α_{1B}-AR from hamsters reports on the specific amino acid residues within the carboxyl tail responsible for each of these processes (36). There are a large number of potential phosphorylation sites in the carboxyl tail of the trout α_{1B}-AR and the other α_1-ARs (Figs. 1–3), suggesting that these receptors too may be subject to desensitization. In fact, one of the putative sites identified in our nucleotide analysis, site 284T, is a phosphorylation domain, so that it is likely that desensitization played some role during the functional divergence between the three α_1-AR subtypes. Together with our measures of relative mRNA expression levels (Fig. 6), these results provide evidence that the differences among the three α_1-AR subtypes impact tissue specificity, ligand specificity, and possibly the signal transduction process and desensitization. Further studies are needed to determine the impact of agonist-induced desensitization of these receptors.

Physiological Differences Between Fish and Mammal α_1-AR Gene Family Members

The position of the G protein binding domains for the trout α_{1A}-, α_{1B}-, and α_{1D}-ARs (Fig. 1–3) is consistent with that previously reported for the trout β_2-AR (26) and the mammalian α_1-ARs and thus appears to be at least partially conserved across the fish and mammalian sequences. Functional implications of differences within this site between the fish and mammalian sequence were not assessed in this study but may result in differences in sensitivity to desensitization during

Downloaded from physiolgenomics.physiology.org on January 7, 2008

Table 5. *Effects of injecting the selective α_{1A}- and α_{1D}-AR antagonists RS-17053 and BMY-7378 on cardiovascular parameters in rainbow trout*

	Preinjection	Catecholamine	Antagonist	Catecholamine
		BMY-7378		
BP, mmHg	22.41±0.36†‡§	40.26±1.85*	18.03±1.54‡	23.78±1.33§
CO, ml·min^{-1}·kg^{-1}	30.35±1.84	34.55±1.27	35.43±2.37	38.83±2.67
R_S, mmHg·ml^{-1}·min^{-1}·kg^{-1}	0.75±0.05†	1.17±0.05*	0.53±0.07†	0.63±0.05†
		RS-17053		
BP, mmHg	22.00±0.44*†	42.96±4.01*	17.18±0.73†	20.92±0.79†
CO, ml·min^{-1}·kg^{-1}	28.24±2.24	37.59±5.04	33.94±3.90	35.72±4.35
R_S, mmHg·ml^{-1}·min^{-1}·kg^{-1}	0.80±0.06†	1.20±0.12*	0.53±0.05†	0.62±0.06†

Basal blood pressure (BP), cardiac output (CO), and system resistance (R_S) were established (preinjection), after which a catecholamine cocktail (2.5×10^{-5} M) was injected (0.6 ml/kg) into the caudal vein cannula; once cardiovascular parameters had stabilized, 0.5 or 1 mg of RS-17053 or BMY-7378 per 900 g fish, respectively, was injected (antagonist). The catecholamine cocktail was again injected following stabilization of the cardiovascular parameters. Peak responses were determined for each parameter after injection. Data are presented as means ± 1SE.; $n = 6$ independent experiments. Values with different symbols are significantly different from each other (across columns only) by 1-way ANOVA followed by Bonferroni.

prolonged agonist exposure. Indeed, receptor phosphorylation is known to be associated with signal turn-off/desensitization and receptor dephosphorylation with resensitization (13).

At the transcript level, the expression profile reported in mammals consistently implicates α_1-ARs in the control of blood pressure (29); we recently demonstrated that the α_{1D}-AR is involved in salt-induced hypertension in trout (7). As in mammals, many trout tissues express multiple α_1-AR subtypes (Fig. 6). Although the reasons for the existence of three α_1-ARs continue to remain elusive, it is thought that the different properties of these receptors result in differential sensitivities to ligands and thus functional differences between vessels (32). In addition, patterns of α_1-AR distribution differ between species and age of the individual and between studies, possibly because of the position within the vascular bed vessels assessed. These observations plus the lack of subtype-specific ligands and the lack of concordance between receptor mRNA and protein hugely complicate the correct identification of the physiologically important receptor type in a particular tissue (20, 24, 32). Although most authors agree that the α_{1A}-AR predominates in most vascular tissues in mammals (20, 32), Marti et al. (24) concluded that, in rats, α_{1D}-ARs predominate in conductance vessels whereas the α_{1A}-ARs predominate in resistance vessels (α_{1B}-ARs play a minor role; Ref. 29). The predominance of the α_{1D}-AR mRNA in the trout vessels studied here is consistent with these rat data, as the trout vessels examined are primarily conductance vessels that are innervated (see Ref. 28). The differences noted between the ABA and EBA in terms of the α_{1D}- and α_{1A}-subtypes are interesting, as changes in these vessels are thought to control blood flow to the gills and thus respiratory exchange (28).

A structure not found in mammals, the BA, receives blood flow from the heart before entering the VA. Although its origin remains in dispute, it is a highly elastic vessel and is known to be innervated by the autonomic nervous system (28). The existence of significant α_{1D}-AR mRNA expression supports this autonomic innervation and adrenergic control over blood flow exiting the heart. The heart itself, however, shows little α_1-AR mRNA. While α_1-ARs play a role in mammalian myocardial contraction (25), the picture in teleost fishes is very species specific. Rainbow trout β-ARs rather than α-ARs are involved in cardiac chronotrophy (28), consistent with the relatively low α_1-AR mRNA expression levels found in the heart (Fig. 6).

In addition to the heart, seven other trout organs were examined for α_1-AR mRNA (Fig. 6). The spleen showed significant α_{1D}- and α_{1B}-AR mRNA, whereas the spleen is a model for the mammalian α_{1B}-AR (43). Contraction of the spleen as a mechanism to increase vascular red blood cell content in fish is controlled by the adrenergic system, but why both receptor subtypes would be present is unknown. The presence of α_{1A}- and α_{1B}-ARs in the whole brain of the trout is again consistent with the importance of these ARs in neural function and especially locomotion (29). Two additional tissues in the trout stand out regarding the relative expression of α_1-ARs, and these are white muscle and liver (Fig. 6). The role of the α_1-AR in white skeletal muscle appears to be unique. Trout liver adrenergic control is primarily through the β_2-AR system, and although prazosin binding is reported in trout hepatocytes, this hepatic α_1-AR is not linked to downstream signaling activity (11). The low expression levels of hepatic α_1-AR mRNA in trout may in part explain its low sensitivity to α-AR agonists compared with the mammalian liver (43). Obviously the functional role of these α_1-ARs in fish tissues requires extensive further study.

To examine the potential role of α_1-ARs in the regulation of blood pressure in trout, cardiovascular parameters were assessed in the presence of α_1-AR selective antagonists. Previous pharmacology studies in mammals demonstrated that BMY-7378 is a high-affinity antagonist for the α_{1D}-AR (18) and that RS-17053 is a high-affinity antagonist of the α_{1A}-AR (15). Both of these antagonists, which were used previously in in vitro experiments with trout (7), inhibited in vivo trout cardiovascular responses (BP, R_S) (Table 5), providing support for the functional existence of both α_{1A}- and α_{1D}-ARs in trout blood vessels and for their potential involvement in the regulation of blood pressure as previously demonstrated (7). Because no significant differences exist between the responses to BMY-7378 and RS-17053, either these drugs are nonselective for the trout α_{1D}- and α_{1A}-ARs or both ARs contribute to regulating blood pressure in vivo. This study was unable to differentiate between these two possibilities. With the use of isolated rings from the ABA and EBA, both BMY-7378 and RS-17053 increased the EC_{50} value for norepinephrine-elicited

Downloaded from physiolgenomics.physiology.org on January 7, 2008

contractions, although the quantitative effects of BMY-7378 were greater, especially in the EBA, inconsistent with the higher prevalence of the α_{1A}-AR mRNA in the tissue (7). Antagonist binding sites have been localized in the mammalian α_1-AR to two clusters of amino acids, one in the second extracellular loop (Gln^{177}-Ile^{178}-Asn^{179}) and two conserved phenylalanine residues (Phe^{308} and Phe^{312}) within TMD7 but close to the extracellular surface (37). These two phenylalanine residues are found in the fish, but only Ile^{178} exists within the second extracellular loop (Fig. 1), although this triplet is apparently less specific than the two phenylalanine residues (37). These two phenylalanine residues also exist within TMD7 of the mammalian and trout α_{1D}-ARs (Fig. 3). If these residues are key to antagonist binding, this may explain the lack of specificity of the two antagonists used in this study. However, the most parsimonious explanation for the results of the two inhibitors is that both α_{1A}- and α_{1D}-ARs contribute to blood pressure control, especially given the relatively wide distribution of these two receptors in trout vessels (Fig. 6).

To conclude, the isolation and cloning of rainbow trout α_1-AR cDNAs represent the initial steps in achieving a better understanding of the entire α_1-adrenergic system in fish and other vertebrates. This study reports on the existence of three members of the trout α_1-AR family, their tissue expression profile, their evolutionary history in the broader context of the α_1-AR gene family, and preliminary data that further support a role for at least the α_{1A}- and α_{1D}-ARs in regulating blood pressure in trout (see also Ref. 7). Although we report only three α_1-ARs, the whole genome duplication experienced by the trout would implicate additional paralogs. These additional paralogs may not have been retained since the split between fish and tetrapods but could have contributed to the functional divergence we report between mammal and fish α_1-ARs. A physiological role for these individual α_1-ARs needs to be defined in fish, taking advantage of the transcript expression pattern seen here between vessels and organs and by expression studies in isolated cells.

GRANTS

This study was supported by grants from the Natural Sciences Research Council of Canada to S. F. Perry, S. Aris-Brosou, and T. W. Moon and by a start-up fund from the University of Ottawa to S. Aris-Brosou.

REFERENCES

1. **Arai K, Tanoue A, Goda N, Takeda M, Takahashi K, Tsujimoto G.** Characterization of the mouse α_{1D}-adrenergic receptor gene. *Jpn J Pharmacol* 81: 271–278, 1999.
2. **Arnold K, Bordoli L, Kopp J, Schwede T.** The SWISS-MODEL workspace: a web-based environment for protein structure homology modelling. *Bioinformatics* 22: 195–201, 2006.
3. **Axelsson M, Fritsche R.** Cannulation techniques. In: *Biochemistry and Molecular Biology of Fishes, Analytical Techniques*, edited by Hochachka PW and Mommsen TP. Amsterdam: Elsevier, 1994, p. 17–32.
4. **Bates PA, Kelley LA, MacCallum RM, Sternberg MJ.** Enhancement of protein modeling by human intervention in applying the automatic programs 3D-JIGSAW and 3D-PSSM. *Proteins Suppl* 5: 39–46, 2001.
5. **Bielawski JP, Yang Z.** A maximum likelihood method for detecting functional divergence at individual codon sites, with application to gene family evolution. *J Mol Evol* 59: 121–132, 2004.
6. **Chalothorn D, McCune DF, Edelmann SE, Garcia-Cazarin ML, Tsujimoto G, Piascik MT.** Differences in the cellular localization and agonist-mediated internalization properties of the α_1-adrenoceptor subtypes. *Mol Pharmacol* 61: 1008–1016, 2002.
7. **Chen X, Moon TW, Olson KR, Dombkowski RA, Perry SF.** The effects of salt-induced hypertension on α_1-adrenoreceptor expression and cardiovascular physiology in the rainbow trout (*Oncorhynchus mykiss*). *Am J Physiol Regul Integr Comp Physiol* 293: R1384–R1392, 2007.
8. **Chen ZJ, Minneman KP.** Recent progress in α_1-adrenergic receptor research. *Acta Pharmacol Sin* 26: 1281–1287, 2005.
9. **Daly CJ, Deighan C, McGee A, Mennie D, Ali Z, McBride M, McGrath JC.** A knockout approach indicates a minor vasoconstrictor role for vascular α_{1B}-adrenoceptors in mouse. *Physiol Genomics* 9: 85–91, 2002.
10. **Fabbri E, Buzzi M, Biondi C, Capuzzo A.** α-Adrenoceptor-mediated glucose release from perifused catfish hepatocytes. *Life Sci* 65: 27–35, 1999.
11. **Fabbri E, Capuzzo A, Gambarotta A, Moon TW.** Characterization of adrenergic receptors and related transduction pathways in the liver of the rainbow trout. *Comp Biochem Physiol* 112B: 643–651, 1995.
12. **Felsenstein J.** *Interferring Phylogenies.* Sunderland, MA: Sinauer, 2003.
13. **Ferguson SS.** Evolving concepts in G protein-coupled receptor endocytosis: the role in receptor desensitization and signaling. *Pharmacol Rev* 53: 1–24, 2001.
14. **Filadelfi AM, Rodrigues PR, Castrucci AM, Visconti MA.** Adrenoceptors in avian and fish pigment cells. *J Comp Physiol* 172B: 599–606, 2002.
15. **Ford AP, Arredondo NF, Blue DR Jr, Bonhaus DW, Jasper J, Kava MS, Lesnick J, Pfister JR, Shieh IA, Vimont RL, Williams TJ, McNeal JE, Stamey TA, Clarke DE.** RS-17053 (N-[2-(2-cyclopropylmethoxyphenoxy)ethyl]-5-chloro-alpha, alpha-dimethyl-1H-indole-3-ethanamine hydrochloride), a selective α_{1A}-adrenoceptor antagonist, displays low affinity for functional α_1-adrenoceptors in human prostate: implications for adrenoceptor classification. *Mol Pharmacol* 49: 209–215, 1996.
16. **Fryxell KJ.** The evolutionary divergence of neurotransmitter receptors and second-messenger pathways. *J Mol Evol* 41: 85–97, 1995.
17. **Gaillard C, Strauss F.** Ethanol precipitation of DNA with linear polyacrylamide as carrier. *Nucleic Acids Res* 18: 378, 1990.
18. **Goetz AS, King HK, Ward SDC, True TA, Rimele TJ, Saussy DL.** Bmy-7378 is a selective antagonist of the D-subtype of α_1-adrenoceptors. *Eur J Pharmacol* 272: R5–R6, 1995.
19. **Goldman N, Yang Z.** A codon-based model of nucleotide substitution for protein-coding DNA sequences. *Mol Biol Evol* 11: 725–736, 1994.
20. **Guimaraes S, Moura D.** Vascular adrenoceptors: an update. *Pharmacol Rev* 53: 451, 2001.
21. **Huelsenbeck JP, Larget B, Alfaro ME.** Bayesian phylogenetic model selection using reversible jump Markov chain Monte Carlo. *Mol Biol Evol* 21: 1123–1133, 2004.
22. **Jordan IK, Rogozin IB, Wolf YI, Koonin EV.** Essential genes are more evolutionarily conserved than are nonessential genes in bacteria. *Genome Res* 12: 962–968, 2002.
23. **Livak KJ, Schmittgen TD.** Analysis of relative gene expression data using real-time quantitative PCR and the $2^{-\Delta\Delta CT}$ method. *Methods* 25: 402–408, 2001.
24. **Marti D, Miquel R, Ziani K, Gisbert R, Ivorra MD, Anselmi E, Moreno L, Villagrasa V, Barettino D, D'Ocon P.** Correlation between mRNA levels and functional role of α_1-adrenoceptor subtypes in arteries: evidence of α_1L as a functional isoform of the α_1A adrenoceptor. *Am J Physiol Heart Circ Physiol* 289: H1923–H1932, 2005.
25. **McCloskey DT, Turnbull L, Swigart P, O'Connell TD, Simpson PC, Baker AJ.** Abnormal myocardial contraction in α_{1A}- and α_{1B}-adrenoceptor double-knockout mice. *J Mol Cell Cardiol* 35: 1207–1216, 2003.
26. **Nickerson JG, Dugan SG, Drouin G, Moon TW.** A putative β_2-adrenoceptor from the rainbow trout (*Oncorhynchus mykiss*). Molecular characterization and pharmacology. *Eur J Biochem* 268: 6465–6472, 2001.
27. **Nielsen R, Yang Z.** Likelihood models for detecting positively selected amino acid sites and applications to the HIV-1 envelope gene. *Genetics* 148: 929–936, 1998.
28. **Olson KR, Farrell AP.** The cardiovascular system. In: *The Physiology of Fishes* (3rd ed.), edited by Evans DH and Claiborne JB. Boca Raton, FL: Taylor and Francis, CRC, 2006, p. 119–152.
29. **Piascik MT, Perez DM.** α_1-Adrenergic receptors: new insights and directions. *J Pharmacol Exp Ther* 298: 403–410, 2001.
30. **Rokosh DG, Simpson PC.** Knockout of the α1A/C-adrenergic receptor subtype: the α1A/C is expressed in resistance arteries and is required to maintain arterial blood pressure. *Proc Natl Acad Sci USA* 99: 9474–9479, 2002.
31. **Ronquist F, Huelsenbeck JP.** MrBayes 3: Bayesian phylogenetic inference under mixed models. *Bioinformatics* 19: 1572–1574, 2003.

Downloaded from physiolgenomics.physiology.org on January 7, 2008

32. **Rudner XL, Berkowitz DE, Booth JV, Funk BL, Cozart KL, D'Amico EB, El-Moalem H, Page SO, Richardson CD, Winters B, Marucci L, Schwinn DA.** Subtype specific regulation of human vascular α_1-adrenergic receptors by vessel bed and age. *Circulation* 100: 2336–2343, 1999.
33. **Soivio A, Nynolm K, Westman K.** Technique for repeated sampling of blood of individual resting fish. *J Exp Biol* 63: 207–217, 1975.
34. **Tanoue A, Nasa Y, Koshimizu T, Shinoura H, Oshikawa S, Kawai T, Sunada S, Takeo S, Tsujimoto G.** The α_{1D}-adrenergic receptor directly regulates arterial blood pressure via vasoconstriction. *J Clin Invest* 109: 765–775, 2002.
35. **Thompson JD, Higgins DG, Gibson TJ.** CLUSTAL W: improving the sensitivity of progressive multiple sequence alignment through sequence weighting, position-specific gap penalties and weight matrix choice. *Nucleic Acids Res* 22: 4673–4680, 1994.
36. **Wang J, Wang L, Zheng J, Anderson JL, Toews ML.** Identification of distinct carboxyl-terminal domains mediating internalization and down-regulation of the hamster α_{1B}-adrenergic receptor. *Mol Pharmacol* 57: 687–694, 2000.
37. **Waugh DJJ, Gaivin RJ, Zuscik MJ, Gonzalez-Cabrera P, Ross SA, Yun J, Perez DM.** Phe-308 and Phe-312 in transmembrane domain 7 are major sites of α_1-adrenergic receptor antagonist binding–imidazoline agonists bind like antagonists. *J Biol Chem* 276: 25366–25371, 2001.
38. **Yang Z.** Maximum likelihood phylogenetic estimation from DNA sequences with variable rates over sites: approximate methods. *J Mol Evol* 39: 306–314, 1994.
39. **Yang Z, Nielsen R.** Codon-substitution models for detecting molecular adaptation at individual sites along specific lineages. *Mol Biol Evol* 19: 908–917, 2002.
40. **Yang Z, Wong WS, Nielsen R.** Bayes empirical Bayes inference of amino acid sites under positive selection. *Mol Biol Evol* 22: 1107–1118, 2005.
41. **Yasuoka A, Abe K, Arai S, Emori Y.** Molecular cloning and functional expression of the α_{1A}-adrenoceptor of medaka fish, *Oryzias latipes*. *Eur J Biochem* 235: 501–507, 1996.
42. **Zhang J, Nielsen R, Yang Z.** Evaluation of an improved branch-site likelihood method for detecting positive selection at the molecular level. *Mol Biol Evol* 22: 2472–2479, 2005.
43. **Zhong H, Minneman KP.** α-Adrenoceptor subtypes. *Eur J Pharmacol* 375: 261–276, 1999.

Downloaded from physiolgenomics.physiology.org on January 7, 2008